Dual systemic tumor targeting with ligand-directed phage and *Grp78* promoter induces tumor regression

Azadeh Kia[1], **Justyna M. Przystal**[1], **Nastasia Nianiaris**[1], **Nicholas D. Mazarakis**[1], **Paul J. Mintz**[2], and **Amin Hajitou**[1]

[1]Gene Therapy, Division of Brain Sciences, Department of Medicine, Imperial College London, Hammersmith Hospital Campus, London W12 0NN, UK

[2]Department of Surgery and Cancer, Imperial College London, Hammersmith Hospital Campus, London W12 0NN, UK

Abstract

The tumor-specific *Grp78* promoter is overexpressed in aggressive tumors. Cancer patients would benefit greatly from application of this promoter in gene therapy and molecular imaging; however, clinical benefit is limited by lack of strategies to target the systemic delivery of *Grp78*-driven transgenes to tumors. This study aims to assess the systemic efficacy of *Grp78*-guided expression of therapeutic and imaging transgenes relative to the standard cytomegalovirus (*CMV)* promoter. Combination of ligand and *Grp78* transcriptional targeting into a single vector would facilitate systemic applications of the *Grp78* promoter. We generated a dual tumor-targeted phage containing the RGD tumor homing ligand and *Grp78* promoter. Next, we combined flow cytometry, western blot, bioluminescence imaging of luciferase and *HSVtk*/ganciclovir gene therapy and compared efficacy to conventional phage carrying the *CMV* promoter *in vitro* and *in vivo* in subcutaneous models of rat and human glioblastoma. We show that double-targeted phage provides persistent transgene expression *in vitro* and in tumors *in vivo* after systemic administration compared to conventional phage. Next, we showed significant tumor killing *in vivo* using the *HSVtk*/ganciclovir gene therapy and found a systemic antitumor effect of *Grp78*-driven *HSVtk* against therapy-resistant tumors. Finally, we uncovered a novel mechanism of *Grp78* promoter activation whereby *HSVtk*/ganciclovir therapy upregulates *Grp78* and transgene expression via the conserved unfolded protein response (UPR) signalling cascade. These data validate the potential of *Grp78* promoter in systemic cancer gene therapy and report the efficacy of a dual tumor targeting phage that may prove useful for translation into gene therapy and molecular imaging applications.

Keywords

targeted cancer therapy; Grp78; tumor targeting

Introduction

Integration of both ligand-directed tropism and transcriptional targeting combined into a single platform could help to facilitate the clinical use of systemic gene therapy and molecular imaging of cancer. The promoter of the glucose-regulated protein 78 (*Grp78*)

Corresponding author: Amin Hajitou, Burlington Danes Building, Hammersmith Hospital Campus, 160 Du Cane Road, London W12 0NN, United Kingdom. Phone: 44-207-594-6546; Fax: 44-207-549-6548; a.hajitou@imperial.ac.uk..

gene, which encodes for an endoplasmic reticulum (ER) chaperone protein, and the ligand RGD that targets αv integrin receptors overexpressed in tumors (1, 2), may offer excellent candidates. The *Grp78* promoter is stress-inducible and is strongly activated by conditions of glucose deprivation, chronic anoxia, and acidic pH that persist within aggressive and poorly perfused tumors (3). Moreover, the *Grp78* promoter is induced in a wide variety of tumours and thus makes it an attractive candidate for use in gene therapy (4-8). Previous studies have clearly demonstrated several advantages of this promoter over viral promoters (9, 10). The safety and tumor specificity of this promoter have also been elegantly reported in transgenic mice carrying a *LacZ* transgene (11). Furthermore, unlike viral promoters used in gene therapy vectors, mammalian promoters such as *Grp78* are not silenced in eukaryotic cells (12). Despite these advantages, the clinical use of the *Grp78* promoter in cancer gene therapy remains hindered. Indeed, transcriptional targeting alone is not sufficient to ensure gene expression in the target cell, but also requires efficient introduction of the *Grp78*-driven expression cassettes after systemic administration. Animal viruses have potential for targeted transgene delivery but require elimination of native tropism for mammalian cells and re-targeting them to alternative receptors (13). A major drawback of these approaches has been the reduced efficacy resulting fromentry via a non-natural receptor (14). Also, incorporation of tumor homing peptide ligands derived from *in vivo* phage display screenings into viral vectors has been attempted, but remains challenging because the strategy can ablate the function of the ligand or disrupt viral assembly and function (14, 15). Our previous work suggests that bacteriophage (phage) - the viruses that infect bacteria only - have the potential to be adapted as targeted delivery vehicles to tumours after systemic administration. We previously reported that the M13-derived phage displaying the double cyclic RGD (CDCRGDCFC, RGD4C) ligand, and carrying an eukaryotic transgene cassette flanked by genomic *cis*-elements of adeno-associated virus (AAV) can selectively deliver transgenes to tumors in rodents after intravenous administration, while sparing the normal organs (14, 16-20). The targeted RGD4C/phage was also used to deliver the tumour necrosis factor-α (TNFα) cytokine to cancers diagnosed in dogs. Repeated therapy with RGD-TNFα proved safe and resulted in complete tumour eradication in a few dogs (21). Consequently, we hypothesized that the RGD4C is a suitable ligand candidate to guide *Grp78*-driven transgene cassettes after systemic administration *in vivo*. We show here our generation of a dual tumor targeting system by using the RGD4C tumor homing ligand and the *Grp78* promoter for transcriptional targeting in the context of bacteriophage. We evaluated this double-targeted phage for gene delivery both *in vitro* and *in vivo*. More specifically, we compared gene expression levels and therapeutic efficacy of our dual targeted phage to those obtained using the conventional phage carrying the cytomegalovirus promoter (*CMV*). We show that the double-targeted vector provides much longer transgene expression than the standard phage *in vitro* and in tumors *in vivo* after intravenous administration to tumor-bearing mice. Additionally, we have identified that the double targeted phage carrying the *Herpes simplex virus-1 thymidine kinase* (*HSVtk*) plus ganciclovir enhances tumor cell killing *in vitro* and produces marked regression of large and therapy-resistant tumors *in vivo* when intravenously administered. Finally, we have uncovered a novel mechanism of *Grp78* promoter induction by *HSVtk* and ganciclovir suicide gene therapy.

Material and Methods

Cell culture

Human Embryonic Kidney (HEK293) cell line was purchased from American Type Culture Collection (ATCC). The U87 and MCF7 cell lines were from the Cancer Research UK and 9L was provided by Dr Hrvoje Miletic, University of Bergen, Norway (22). No authentication of cells was done by the authors. All cell lines were maintained in DMEM supplemented with foetal bovine serum, L-glutamine, penicillin and streptomycin. Stress

experiments were performed with either 300 nM TG for 16 hr or 0.5 µM A23187 for 5 hr. Ganciclovir (GCV) was used at 20µmol/L and renewed daily.

Vector construction and phage production

To generate the double-targeted phage displaying the RGD4C ligand and carrying the *Grp78* promoter, the 689bp fragment containing the rat *Grp78* promoter was released from pDrive-rGRP78 plasmid (Invivogen) by *Pst*I and *Nco*I digestion, then ligated to *Xba*I linkers and subsequently inserted into *Xba*I site of pBluescript II. The pBluescript II plasmid was then used to release the *Grp78* promoter by *Spe*I and *Not*I followed by ligation to the phage vector plasmid digested with *Nhe*I and *Not*I to replace the *CMV* promoter (*Spe*I can ligate to *Nhe*I). Phage viral particles were amplified as described (18) then expressed as transducing units (TU/µl).

Western blot

Whole cell lysates were prepared in RIPA buffer and subjected to immunoblot. We used goat anti-Grp78 (C-20, 1:400) and mouse anti-GAPDH (6C5, 1:1000) from Santa Cruz Biotechnology, rabbit anti-HSVtk (1:100) from Dr. William Summers (Yale university, USA), mouse anti-ATF6 (IMG-273, 5 µg/ml) from Imgenex-USA and rabbit-anti phosphor-eIF2α (1:1000) from Cell Signalling. Each immunoblot was done three times, quantified by ImageJ software and normalized to GAPDH.

XBP1 splicing measurement

To detect unspliced and spliced forms of the x-box binding protein 1 (*XBP1)*, semi-quantitative RT-PCR was performed as described (23).

Animal models and antitumor therapy of *HSVtk*/GCV

To establish tumors in mice, a total of 1×10^6 9L or 1×10^7 U87 cells were subcutaneously implanted into immunodeficient nude mice. Mice were anesthetised by gas (2% isoflurane and 98% oxygen) inhalation. Tumor-bearing mice were intravenously administered through the tail vein with targeted or control insertless vectors carrying the *HSVtk* at a dose of 5×10^{10} TU vector /mouse as we reported (17, 18). GCV (70 mg/kg/day), intraperitoneal, was given to mice as indicated in the figures. Tumor growth was monitored three times a week by calliper measurements and tumor volumes were calculated as described (7, 16, 17). All *in vivo* experiments were carried out according to the Institutional and Home Office Guidelines. We have used 6 mice per group and repeated the experiments three times. However, in some therapy experiments involving mice with large tumors, we have repeated the experiments three times with the minimal number of animals per group to reduce animal suffering and apply the 3Rs ("Reduce, Refine and Replace") in accordance with the Institutional and Home Office guidelines.

In vivo bioluminescence imaging (BLI)

To monitor *Luc* expression, mice were anesthetized and administered with 100 mg/kg of d-luciferin (Gold Biotechnology), then imaged using the *In Vivo* Imaging System (IVIS 100) (Caliper Life Sciences). A region of interest (ROI) was defined manually over the tumors for measuring signal intensities recorded as total photon counts per second per cm^2 (photons/sec/cm^2/sr).

Statistical analyses

We used GraphPad Prism software (version 5.0). Error bars represent standard error of the mean (s.e.m). P values were generated by ANOVA and denoted as: *$p<0.05$, **$p<0.01$ and ***$p<0.001$.

Results

Ligand-directed and transcriptional-targeted RGD4C/*Grp78* particles are functional

As a proof of concept, we generated a double targeted phage viral particle consisting of the rat *Grp78* promoter and phage displaying the RGD4C ligand. We used the *Grp78* of rat because the promoter sequences of *Grp78* are highly conserved among rodents and humans (24, 25), and this promoter is active in a wide range of species including human and murine (10, 11). To obtain the double targeted phage (hereafter referred to as RGD4C/*Grp78*), we replaced the *CMV* promoter in the RGD4C phage (hereafter referred to as RGD4C/*CMV*) with the *Grp78* promoter. As a control we replaced the *CMV* promoter of the insertless phage (non-targeted) with the *Grp78* (Supplementary Fig. S1). To show that the *Grp78* promoter retains its inducible function in the context of the double targeted phage, we transduced the αv integrin-expressing HEK293 cells with RGD4C/*Grp78-GFP*, and showed that treatment with thapsigargin (TG), a standard inducer of *Grp78*, induced GFP expression relative to non-treated cells (Supplementary Fig. S2). We also confirmed these findings with calcium ionophore A23187, as an additional inducer of *Grp78* promoter (Supplementary Fig. S2). No GFP expression was detected with control non-targeted *Grp78-GFP* and either TG or A23187. These data establish that (i) the ligand-directed transduction by RGD4C and (ii) the stress-inducible property of *Grp78* promoter are intact and functional in the context of the dual targeted phage.

RGD4C/*Grp78* provides long-term transgene expression in tumor cells

We conducted transgene expression analyses and all subsequent studies in models of glioblastoma since this tumor remains a challenge to treat in patients. We used the rapidly growing 9L rat glioblastoma cells because *Grp78* is known to be highly active in aggressive tumors (26-28). Additionally, we evaluated efficacy in the U87 human glioblastoma cells characterized by being moderately aggressive (29). We carried out an *in vitro* characterization of these cell lines and observed a higher proliferation rate in 9L cells relative to U87 (Supplementary Fig. S3A) and better survival in low serum conditions (Supplementary Fig. S3B). Moreover, western blot analysis showed increased levels of endogenous Grp78 in 9L as compared to U87 cells (Supplementary Fig. S3C). RT-PCR experiments revealed the presence of the spliced form of the messenger RNA (mRNA) of the *XBP1* in the 9L cells, while it was induced in U87 cells upon TG treatment only (Supplementary Fig. S3D). This spliced mRNA is translated into the functional XBP1 protein, which acts as a transcription factor for the *Grp78* promoter.

We next set out to determine efficacy of transgene expression mediated by the RGD4C/*Grp78* in 9L and U87 tumor cells. Stably transduced cells were generated by using vectors carrying *puro^R* that confers resistance to puromycin. Either RGD4C/*Grp78-GFP-puro^R* or RGD4C/*CMV-GFP-puro^R* were used to transduce 9L and U87 cells and clones were isolated under puromycin selection. Firstly, we counted and monitored GFP positive cell clones. Although cell clones transduced with RGD4C/*CMV-GFP-puro^R* retained resistance to puromycin, GFP expression was generally weaker over time than that of the RGD4C/*Grp78-GFP-puro^R* clones. At day 14 post-vector transduction (Fig. 1A) we observed GFP expression in 92% of the 9L clones transduced by the RGD4C/*Grp78-GFP-puro ^R* construct (n= 846 of 959 clones), compared to 83% of clones transduced by RGD4C/*CMV-GFP-puro^R* (n= 845 of 1258 clones). At day 28 post-transduction, we detected GFP in 83% of RGD4C/*Grp78-GFP-puro ^R* 9L clones, while only 59% of the clones transduced by RGD4C/*CMV-GFP-puro^R* had GFP positive cells (Fig. 1A). We also observed 67.4 % of the U87 clones transduced by RGD4C/*Grp78-GFP-puro^R* contained GFP positive cells (n= 177 of 276 clones) compared to only 47.3% (n=126 of 300 clones) of clones transduced with RGD4C/*CMV-GFP-puro^R* at day 17 post-transduction (Fig. 1A). No further significant

change in GFP was observed in U87 cell clones at day 31 post-transduction with either vector.

To confirm persistence of transgene expression by RGD4C/*Grp78-GFP*, all cell clones were pooled and GFP expression analyzed by flow cytometry. At day 39 post-vector transduction, 57% of 9L cells transduced by RGD4C/*Grp78-GFP* were positive for GFP expression and this number increased drastically to 85% at day 97 (Fig. 1B). In contrast, only 37% of cells transduced by the RGD4C/*CMV-GFP* expressed GFP at day 39, followed by a considerable drop to 11% at day 97 (Fig. 1B). Furthermore, we observed ~10 fold drop of the mean fluorescent intensity (MFI) of RGD4C/*CMV-GFP* cells, while the MFI remained stable in cells transduced with RGD4C/*Grp78-GFP*.

Similarly, FACS analyses showed that GFP expression in U87 cells transduced by RGD4C/*Grp78-GFP* increased from 37% at day 39 to 66.3% at day 75 post-transduction (Fig. 1C). In contrast, although cells transduced with RGD4C/*CMV-GFP* had 59% GFP positive cells at day 39, this number decreased remarkably to 5.6% at day 75 post-transduction (Fig. 1C). Moreover, while U87 cells transduced with RGD4C/CMV-*GFP* presented significantly higher MFI than RGD4C/*Grp78-GFP* cells at day 39, their MFI decreased by ~18 fold at day 75 post-transduction.

Next, we sought to confirm the improved transgene expression in RGD4C/*Grp78*-transduced cells over time in an *in vivo* context. 9L cells stably transduced with RGD4C/*Grp78* or RGD4C/*CMV* vectors expressing the firefly luciferase reporter transgene (*Luc*) were subcutaneously implanted into immunodeficient nude mice. *Luc* expression was monitored in tumors by repetitive bioluminescence imaging (BLI) of tumor-bearing mice (Supplementary Fig. S4A). While *Luc* expression was comparable between the two groups within the initial tumor growth phase, it increased significantly over time in tumors derived from RGD4C/*Grp78*-transduced cells compared to RGD4C/*CMV*-derived tumors (Supplementary Fig. S4B).

RGD4C/*Grp78-HSVtk* plus GCV treatment produces strong and constant tumor cell killing

To test tumor cell killing efficacy, we constructed the RGD4C/*Grp78-HSVtk* encoding the *HSV1tk* mutant SR39 (30) and compared with the RGD4C/*CMV-HSVtk* construct. The *HSVtk* gene can serve as a suicide gene when combined with GCV. Tumor cells were transduced with RGD4C/*Grp78-HSVtk-Puro^R* or RGD4C/*CMV-HSVtk-Puro^R* to generate stably transduced cells. *HSVtk* expression was assessed over a time course by western blot. Consistent with FACS experiments, *HSVtk* expression in 9L cells transduced by RGD4C/*Grp78* was significantly higher and increased gradually over time than in cells transduced with RGD4C/*CMV-HSVtk* (Fig. 2A). In contrast, a dramatic decrease of *HSVtk* levels was observed in cells transduced with RGD4C/*CMV-HSVtk* towards day 78 post-transduction (Fig. 2A). In U87 cells, and consistent with the MFI results, although *HSVtk* expression was initially stronger in cells transduced with RGD4C/*CMV-HSVtk*, it decreased gradually overtime, while *HSVtk* remained constant in cells transduced with RGD4C/*Grp78-HSVtk* (Fig. 2B).

We next set out to assess tumor cell killing *in vitro* by vectors for days 47 (t1) and 109 (t2) post-transduction. *HSVtk* gene therapy was induced at each time point by GCV treatment for 24hr, 48hr, 72hr or 96 hr. Addition of GCV at t1 resulted in significantly higher death of 9L cells by RGD4C/*Grp78-HSVtk* than RGD4C/*CMV-HSVtk* (Fig. 2 C and D). Importantly, we observed a rapid decrease in the efficacy of tumor cell killing by RGD4C/*CMV-HSVtk* at t2, while efficacy of RGD4C/*Grp78-HSVtk* remained stable overtime consistent with western blot analysis of *HSVtk* expression (Fig. 2A).

Surprisingly, in U87 cells, there was no significant difference between RGD4C/*Grp78-HSVtk* and RGD4C/*CMV-HSVtk* vectors in cell death induction by GCV at day 66 (t1) post-transduction (Supplementary Fig. S5), although *HSVtk* expression was higher in cells transduced by the RGD4C/*CMV-HSVtk* as shown in Fig. 2B.

Because RGD4C/*Grp78* vector has been designed for systemic gene therapy *in vivo*, we sought to examine whether the persistence of transgene expression by RGD4C/*Grp78* occurs in unselected transduced cells. Thus, transduction in the absence of puromycin selection showed better persistence over time of *Luc* transgene expression by the RGD4C/*Grp78-Luc* compared to RGD4C/*CMV-Luc* (Supplementary Fig. S6A). Furthermore, the tumor cell killing effect of the RGD4C/*Grp78-HSVtk* in both 9L and U87 cells proved more efficient than that of the RGD4C/*CMV-HSVtk* as measured at day 9 post-transduction (Supplementary Fig. S6B and S6C).

To rule out the possibility that the activity of *Grp78* promoter is tumor cell specific, we assessed efficiency of RGD4C/*Grp78* in the MCF7 human breast cancer cells in the absence of puromycin selection. The basal *Grp78* promoter activity was initially low following transduction of MCF7 cells; importantly however this activity increased overtime and was further induced by stressing the cells with TG treatment that resulted in 2.2 fold increase toward day 10 post-transduction (Supplementary Fig. S7A). Consistently, western blot analysis confirmed induction of the endogenous *Grp78* gene by TG treatment (Supplementary Fig. S7B).

Systemic tumor targeting of gene delivery by the RGD4C/*Grp78*

Next, we evaluated the specificity and efficacy of gene delivery in tumors after systemic administration of RGD4C/*Grp78* and compared this alongside RGD4C/*CMV*. As an initial preclinical model, we used immunodeficient nude mice bearing subcutaneous tumors derived from 9L cells. We first used *in vivo* BLI of the *Luc* transgene reporter (31, 32) after a single intravenous administration of RGD4C/*Grp78-Luc*, RGD4C/*CMV-Luc*, or control insertless vectors in tumor-bearing mice. *Luc* expression within 9L tumors was detectable at day 3 after RGD4C/*CMV-Luc* administration (Fig. 3A and 3B) with a linear increase to reach maximum transgene expression at day 5 that lasted only briefly, followed by a rapid decrease. In sharp contrast, a significantly higher tumor expression of *Luc* was achieved at day 3 by RGD4C/*Grp78-Luc*, followed by gradual and much longer stabilization of *Luc* expression towards day 7 (Fig. 3A and 3B). Finally, no tumor-associated bioluminescent signals were observed with control vectors, and no bioluminescence was observed in normal organs from all experimental groups.

In a second set of experiments, we used the RGD4C/*Grp78* encoding the *HSVtk* to determine therapeutic efficacy. Cohorts of mice bearing 9L tumors (~100 mm^3) received a single intravenous dose of RGD4C/*Grp78-HSVtk*, RGD4C/*CMV-HSVtk*, or control vectors followed by GCV treatment in all groups at day 3 post-vector delivery. Tumor size (Fig. 3C) and tumor viability (Fig. 3D) were evaluated. Similar tumor growth suppressive effects were initially observed with GCV treatment of mice receiving RGD4C/*Grp78-HSVtk* or RGD4C/*CMV-HSVtk* as compared to mice treated with control vectors (Fig. 3C). However, when tumors grew back after therapy, repeated treatment with GCV resulted in tumour growth inhibition in mice that received RGD4C/*Grp78-HSVtk* (Fig. 3C). In contrast, GCV had little to no effect on the large tumors treated with RGD4C/*CMV-HSVtk* therapy. Moreover, RGD4C/*Grp78-HSVtk* was associated with superior suppressive effects on tumor viability compared with RGD4C/*CMV-HSVtk* as assessed with BLI of *Luc* expression in tumors (Fig. 3D).

To rule out the possibility that the observed antitumor effects were tumor specific, we analysed efficacy of RGD4C/*Grp78-HSVtk* on the U87-derived xenografts. Similar antitumor effects seen in the 9L tumors were initially detected in the U87 xenografts following GCV treatment of mice administered with single doses of either RGD4C/*Grp78-HSVtk* or RGD4C/*CMV-HSVtk* as compared to control mice injected with control vectors (Fig. 4A and 4B). Yet again, when tumors grew back after therapy, repeated GCV treatment resulted in a sharp regression of tumor volumes in mice that received the RGD4C/*Grp78-HSVtk* as compared to mice receiving RGD4C/*CMV-HSVtk* (Fig. 4A and 4B). Additionally, tumor viability was markedly suppressed in tumors from mice injected with the RGD4C/*Grp78-HSVtk* vector as evidenced by loss of *Luc* activity (Fig. 4C).

Systemic administration of RGD4C/*Grp78-HSVtk* and GCV induces regression of large tumors

To confirm the therapeutic advantage of RGD4C/*Grp78* in treating large and rapidly growing tumors, we evaluated RGD4C/*Grp78-HSVtk* in large 9L tumors. First, to monitor *Grp78* activity during tumor growth prior to GCV treatment, we generated 9L cells stably expressing the *Luc* transgene under the *Grp78* promoter. Next, 9L/*Grp78-Luc* cells were implanted subcutaneously into nude mice, then RGD4C/*Grp78-HSVtk*, RGD4C/*CMV-HSVtk*, or control vectors were intravenously injected when tumors reached large volumes (~250-300 mm^3). At day 3 post-vector injection, tumors grew rapidly to reach large size (~400-450 mm^3) and BLI of *Luc* expression revealed high activity of the *Grp78* promoter within tumors (Fig. 5A). We therefore initiated GCV treatment at day 3 post-vector injection and after 5 days, the double targeted RGD4C/*Grp78-HSVtk* vector induced a marked regression of the large tumors compared to mice injected with RGD4C/*CMV-HSVtk* (Fig. 5A and 5B). Moreover, no effect on tumor growth was observed in mice treated with control vectors. Hematoxylin and eosin (H&E) staining revealed extensive cell death in tumors by RGD4C/*Grp78-HSVtk* plus GCV (Fig. 5C). In contrast, RGD4C/*CMV-HSVtk* and control vectors had no such effect.

Suicide gene therapy with *HSVtk* and GCV increases endogenous *Grp78* promoter activity and boosts transgene expression mediated by RGD4C/*Grp78*

To gain further insight into the efficacy the double targeted RGD4C/*Grp78-HSVtk*, we investigated the effect of the *HSVtk* plus GCV therapy on the activity of *Grp78* promoter at both levels endogenous *Grp78* and RGD4C/*Grp78* vector. 9L cells stably transduced with RGD4C/*Grp78-HSVtkpuro^R* or RGD4C/*CMV-HSVtk-puro^R* were treated with GCV for 1hr to12hr. Western blot analyses showed a gradual increase of endogenous Grp78 levels, ~3-fold increase by 12 hr, with GCV treatment of 9L cells transduced with both RGD4C/*Grp78-HSVtk-puro^R* or RGD4C/*CMV-HSVtk-puro^R* (Fig. 6A and 6B). In contrast HSVtk levels were only increased by GCV in cells transduced by RGD4C/*Grp78-HSVtk-puro^R*, ~2.5-fold at 12 hr (Fig. 6A), while no effect of GCV on HSVtk expression was observed in cells transduced with RGD4C/*CMV-HSVtk-puro^R* (Fig. 6B). These data confirm that HSVtk/GCV therapy activates both promoters of endogenous *Grp78* and of the RGD4C/*Grp78* vector.

We then checked whether *Grp78* activation by HSVtk/GCV is mediated through the conserved signalling cascade termed UPR pathway that regulates the *Grp78* (33-35). Thus, we investigated three ER transmembrane proteins representing the three arms of the UPR pathway (33-35). We first assessed the protein kinase- like ER kinase (PERK). Upon dissociation of Grp78, PERK homooligomerizes and phosphorylates the eukaryotic initiation factor 2α (eIF2α) that selectively promotes translation of the transcription factor ATF4 which induces the *Grp78* promoter (35). Western blot analyses showed that GCV induces the phospho-eIF2α which is detectable at 9hr post GCV treatment (Fig. 6C).

Next, we found that GCV increases the 90-kDa form of the activating transcription factor 6 (ATF6), which became evident at 6 hr post GCV treatment (Fig. 6D). Previous studies have shown that the PERK/phosphorylated-eIF2α pathway can activate and control ATF6 expression in response to ER stress (35). An increase in the 90-kDa ATF6 level after GCV treatment further demonstrates initiation of the ER stress pathway and subsequently activation of UPR.

Finally, upon dissociation of Grp78, activated inositol requiring enzyme 1 (IRE1) splices the mRNA of *XBP1* (33). RT-PCR analyses show that this mRNA was constitutively spliced in 9L cells (Supplementary Fig. S8) and that GCV treatment had no further effect.

Discussion

The RGD4C/*Grp78* phage is a promising gene transfer tool that implements ligand-directed and transcriptional targeting into a single vector. Our studies here are the first to report efficacy of systemic gene delivery with the *Grp78* promoter, and establish the double targeted RGD4C/*Grp78* as superior to the conventional RGD4C/*CMV* phage in providing striking persistence of gene expression *in vitro* and *in vivo* and a clear advantage in *HSVtk* and GCV systemic cancer gene therapy. It has been reported that in comparison with the murine leukemia LTR viral promoter, *Grp78*-regulated suicide cancer gene therapy is stronger (9). Our studies are the first to compare *Grp78* to the commonly utilized *CMV* viral promoter *in vitro* and *in vivo*, and further prove the superiority of *Grp78* to a viral promoter in cancer gene therapy, in particular when both promoters are systemically targeted to tumors. The *in vitro* cell killing advantage of RGD4C/*Grp78* is supported by our reporter transgene expression studies and western blot analysis of *HSVtk* showing persistence of gene expression by *Grp78* and silencing of the *CMV* promoter. These data are consistent with numerous reports showing that the *CMV* promoter undergoes silencing *in vitro* and *in vivo* by mammalian host cells (12, 36, 37). Our observations following analysis of *HSVtk*/ GCV killing of U87 cells merit further discussion. It is important to note that overall activity of the *Grp78* promoter is low in this cell line, these cells are under less ER stress, and the proliferation rate of U87 cells is lower than that of 9L cells. A positive correlation between cell proliferation rate and *Grp78* activity has been reported (28). Interestingly, similar cell death was induced by RGD4C/*Grp78-HSVtk* than RGD4C/*CMV-HSVtk*. One possible explanation is while U87 cells were not subjected to stress in gene expression analysis, those expressing *HSVtk* may have experienced ER stress following GCV treatment. Finally, we confirmed the efficiency of RGD4C/*Grp78* in another model of the MCF7 human breast cancer. Overexpression of *Grp78* gene was previously reported in human malignant breast cancer but not in benign breast lesions (27). Consistently, the activity in MCF7 was increased upon stress induction with TG treatment, indicating that the stress-inducible *Grp78* promoter of RGD4C/*Grp78* is active in different tumor types and is induced under conditions that persist within aggressive tumors (3).

In vivo, systemic administration of the RGD4C/*Grp78* initiates higher transgene expression with a more stable pattern than the RGD4C/*CMV*. The drop of *Luc* expression observed with both RGD4C/*CMV-Luc* and, at a later time point, with RGD4C/*Grp78-Luc*, could be explained by dilution effects of proliferating transduced cells within a larger population of proliferating non-transduced cells. However, comparable antitumor effects were obtained at early time points on small tumors, which could be due to the bystander effect of the *HSVtk*/ GCV (20). Importantly, we demonstrated the antitumor effect of RGD4C/*Grp78* on large 9L tumors consistently with specific activation of the *Grp78* promoter in poorly perfused malignant tissues, including tumor-associated vasculature and tumor cells (38). Moreover, we report an antitumor effect of RGD4C/*Grp78* on recurrent tumors, which can be explained by i) *Grp78* being a stress-inducible gene that encodes for a potent anti-apoptotic protein

that plays a critical role in tumor survival and resistance to therapy, ii) specific over-activation of *Grp78* in aggressive cancers, and iii) our findings that *HSVtk*/GCV stimulates the UPR stress pathway leading to increased *Grp78* activity. Recent studies have shown that chemotherapeutic drugs stimulate *Grp78* expression (26). Yet, this is the first report to show that *HSVtk*/GCV gene therapy activates *Grp78* at both endogenous and vector levels. In this manner, cells transduced by RGD4C/*Grp78-HSVtk* unintentionally facilitate their own death upon GCV treatment by activating the UPR stress pathway and ultimately *Grp78*. These data are also consistent with previous work reporting the stronger tumor cell killing efficacy of *HSVtk* under the *Grp78* promoter in comparison to viral promoters. Accordingly, our studies provide the proof-of-concept for taking advantage of a cancer cell's own resistant mechanisms in order to enhance gene therapy against therapy-resistant tumors.

In conclusion, RGD4C/*Grp78* holds the potential to treat large and therapy resistant tumors after systemic administration. Our dual targeting platform further ensures selective transgene transfer to tumors. Moreover, our studies show the efficacy of combining homing ligands and a mammalian tumor-specific promoter in the context of bacteriophage. This vector could also enhance the effectiveness of molecular-genetic imaging. The translation of the double-targeted RGD4C/*Grp78* particle may lead to clinical applications of the *Grp78* promoter.

Supplementary Material

Refer to Web version on PubMed Central for supplementary material.

Acknowledgments

ABBREVIATION LIST

AAVP	Adeno-associated virus/Phage
ATF6	Activating transcription factor 6
CMV	Cytomegalovirus
eIF2α	Eukaryotic initiation factor 2α
GCV	Ganciclovir
GFP	Green fluorescent protein
Grp78	Glucose-regulated protein 78
HSVtk	Herpes Simplex Virus thymidine kinase
IRE1	Inositol requiring enzyme 1
ITRs	Inverted terminal repeats
PERK	Protein kinase-like ER kinase
UPR	Unfolded protein response

XBP1   X-box binding protein 1

References

1. Ellerby HM, Arap W, Ellerby LM, Kain R, Andrusiak R, Rio GD, et al. Anti-cancer activity of targeted pro-apoptotic peptides. Nat Med. 1999; 5:1032–8. [PubMed: 10470080]

2. Arap W, Pasqualini R, Ruoslahti E. Cancer treatment by targeted drug delivery to tumor vasculature in a mouse model. Science. 1998; 279:377–80. [PubMed: 9430587]

3. Li J, Lee AS. Stress induction of GRP78/BiP and its role in cancer. Curr Mol Med. 2006; 6:45–54. [PubMed: 16472112]

4. Lee AS. GRP78 induction in cancer: therapeutic and prognostic implications. Cancer Res. 2007; 67:3496–9. [PubMed: 17440054]

5. Song MS, Park YK, Lee JH, Park K. Induction of glucose-regulated protein 78 by chronic hypoxia in human gastric tumor cells through a protein kinase C-epsilon/ERK/AP-1 signaling cascade. Cancer Res. 2001; 61:8322–30. [PubMed: 11719466]

6. Shuda M, Kondoh N, Imazeki N, Tanaka K, Okada T, Mori K, et al. Activation of the ATF6, XBP1 and grp78 genes in human hepatocellular carcinoma: a possible involvement of the ER stress pathway in hepatocarcinogenesis. J Hepatol. 2003; 38:605–14. [PubMed: 12713871]

7. Arap MA, Lahdenranta J, Mintz PJ, Hajitou A, Sarkis AS, Arap W, et al. Cell surface expression of the stress response chaperone GRP78 enables tumor targeting by circulating ligands. Cancer Cell. 2004; 6:275–84. [PubMed: 15380518]

8. Koomagi R, Mattern J, Volm M. Glucose-related protein (GRP78) and its relationship to the drug-resistance proteins P170, GST-pi, LRP56 and angiogenesis in non-small cell lung carcinomas. Anticancer Res. 1999; 19:4333, 6. [PubMed: 10628396]

9. Azatian A, Yu H, Dai W, Schneiders FI, Botelho NK, Lord RV. Effectiveness of HSV-tk suicide gene therapy driven by the Grp78 stress-inducible promoter in esophagogastric junction and gastric adenocarcinomas. J Gastrointest Surg. 2009; 13:1044–51. [PubMed: 19277794]

10. Chen X, Zhang D, Dennert G, Hung G, Lee AS. Eradication of murine mammary adenocarcinoma through HSVtk expression directed by the glucose-starvation inducible grp78 promoter. Breast Cancer Res Treat. 2000; 59:81–90. [PubMed: 10752683]

11. Dong D, Dubeau L, Bading J, Nguyen K, Luna M, Yu H, et al. Spontaneous and controllable activation of suicide gene expression driven by the stress-inducible grp78 promoter resulting in eradication of sizable human tumors. Hum Gene Ther. 2004; 15:553–61. [PubMed: 15212714]

12. Brooks AR, Harkins RN, Wang P, Qian HS, Liu P, Rubanyi GM. Transcriptional silencing is associated with extensive methylation of the CMV promoter following adenoviral gene delivery to muscle. J Gene Med. 2004; 6:395–404. [PubMed: 15079814]

13. Allen C, Vongpunsawad S, Nakamura T, James CD, Schroeder M, Cattaneo R, et al. Retargeted oncolytic measles strains entering via the EGFRvIII receptor maintain significant antitumor activity against gliomas with increased tumor specificity. Cancer Res. 2006; 66:11840–50. [PubMed: 17178881]

14. Hajitou A. Targeted systemic gene therapy and molecular imaging of cancer contribution of the vascular-targeted AAVP vector. Adv Genet. 2010; 69:65–82. [PubMed: 20807602]

15. Ghosh D, Barry MA. Selection of muscle-binding peptides from context-specific peptide-presenting phage libraries for adenoviral vector targeting. J Virol. 2005; 79:13667–72. [PubMed: 16227286]

16. Hajitou A, Lev DC, Hannay JA, Korchin B, Staquicini FI, Soghomonyan S, et al. A preclinical model for predicting drug response in soft-tissue sarcoma with targeted AAVP molecular imaging. Proc Natl Acad Sci USA. 2008; 105:4471–6. [PubMed: 18337507]

17. Hajitou A, Trepel M, Lilley CE, Soghomonyan S, Alauddin MM, Marini FC, et al. A hybrid vector for ligand-directed tumor targeting and molecular imaging. Cell. 2006; 125:385–98. [PubMed: 16630824]

18. Hajitou A, Rangel R, Trepel M, Soghomonyan S, Gelovani JG, Alauddin MM, et al. Design and construction of targeted AAVP vectors for mammalian cell transduction. Nat Protoc. 2007; 2:523–31. [PubMed: 17406616]

19. Tandle A, Hanna E, Lorang D, Hajitou A, Moya CA, Pasqualini R, et al. Tumor vasculature-targeted delivery of tumor necrosis factor-alpha. Cancer. 2009; 115:128–39. [PubMed: 19090007]

20. Trepel M, Stoneham CA, Eleftherohorinou H, Mazarakis ND, Pasqualini R, Arap W, et al. A heterotypic bystander effect for tumor cell killing after adeno-associated virus/phage-mediated, vascular-targeted suicide gene transfer. Mol Cancer Ther. 2009; 8:2383–91. [PubMed: 19671758]

21. Paoloni MC, Tandle A, Mazcko C, Hanna E, Kachala S, Leblanc A, et al. Launching a novel preclinical infrastructure: comparative oncology trials consortium directed therapeutic targeting of TNFalpha to cancer vasculature. PLoS One. 2009; 4:e4972. [PubMed: 19330034]

22. Miletic H, Fischer YH, Giroglou T, Rueger MA, Winkeler A, Li H, et al. Normal brain cells contribute to the bystander effect in suicide gene therapy of malignant glioma. Clin Cancer Res. 2007; 13:6761–8. [PubMed: 18006778]

23. Samali A, Fitzgerald U, Deegan S, Gupta S. Methods for monitoring endoplasmic reticulum stress and the unfolded protein response. Int J Cell Biol. 2010; 2010:830307. [PubMed: 20169136]

24. Ting J, Lee AS. Human gene encoding the 78,000-dalton glucose-regulated protein and its pseudogene: structure, conservation, and regulation. DNA. 1988; 7:275–86. [PubMed: 2840249]

25. Resendez E Jr, Wooden SK, Lee AS. Identification of highly conserved regulatory domains and protein-binding sites in the promoters of the rat and human genes encoding the stress-inducible 78-kilodalton glucose-regulated protein. Mol Cell Biol. 1988; 8:4579–84. [PubMed: 3185564]

26. Pyrko P, Schonthal AH, Hofman FM, Chen TC, Lee AS. The unfolded protein response regulator GRP78/BiP as a novel target for increasing chemosensitivity in malignant gliomas. Cancer Res. 2007; 67:9809–16. [PubMed: 17942911]

27. Fernandez PM, Tabbara SO, Jacobs LK, Manning FC, Tsangaris TN, Schwartz AM, et al. Overexpression of the glucose-regulated stress gene GRP78 in malignant but not benign human breast lesions. Breast Cancer Res Treat. 2000; 59:15–26. [PubMed: 10752676]

28. Lee HK, Xiang C, Cazacu S, Finniss S, Kazimirsky G, Lemke N, et al. GRP78 is overexpressed in glioblastomas and regulates glioma cell growth and apoptosis. Neuro Oncol. 2008; 10:236–43. [PubMed: 18403493]

29. Dos Santos C, Karaky R, Renoir D, Hamma-Kourbali Y, Albanese P, Gobbo E, et al. Antitumorigenic effects of a mutant of the heparin affin regulatory peptide on the U87 MG glioblastoma cell line. Int J Cancer. 2010; 127:1038–51. [PubMed: 20013808]

30. Black ME, Kokoris MS, Sabo P. Herpes simplex virus-1 thymidine kinase mutants created by semi-random sequence mutagenesis improve prodrug-mediated tumor cell killing. Cancer Res. 2001; 61:3022–6. [PubMed: 11306482]

31. Keyaerts M, Heneweer C, Gainkam LO, Caveliers V, Beattie BJ, Martens GA, et al. Plasma protein binding of luciferase substrates influences sensitivity and accuracy of bioluminescence imaging. Mol Imaging Biol. 2011; 13:59–66. [PubMed: 20383591]

32. Huang R, Vider J, Serganova I, Blasberg RG. Atp-binding Cassette Transporters Modulate Both Coelenterazine- And d-luciferin-based Bioluminescence Imaging. Mol Imaging. 2012; 11:1–12.

33. Hetz C, Martinon F, Rodriguez D, Glimcher LH. The unfolded protein response: integrating stress signals through the stress sensor IRE1alpha. Physiol Rev. 2011; 91:1219–43. [PubMed: 22013210]

34. Zhang LH, Zhang X. Roles of GRP78 in physiology and cancer. J Cell Biochem. 2010; 110:1299–305. [PubMed: 20506407]

35. Teske BF, Wek SA, Bunpo P, Cundiff JK, McClintick JN, Anthony TG, et al. The eIF2 kinase PERK and the integrated stress response facilitate activation of ATF6 during endoplasmic reticulum stress. Mol Biol Cell. 2011; 22:4390–405. [PubMed: 21917591]

36. Grassi G, Maccaroni P, Meyer R, Kaiser H, D'Ambrosio E, Pascale E, et al. Inhibitors of DNA methylation and histone deacetylation activate cytomegalovirus promoter-controlled reporter gene expression in human glioblastoma cell line U87. Carcinogenesis. 2003; 24:1625–35. [PubMed: 12869421]

37. Prosch S, Stein J, Staak K, Liebenthal C, Volk HD, Kruger DH. Inactivation of the very strong HCMV immediate early promoter by DNA CpG methylation in vitro. Biol Chem Hoppe Seyler. 1996; 377:195–201. [PubMed: 8722321]

38. Virrey JJ, Dong D, Stiles C, Patterson JB, Pen L, Ni M, et al. Stress chaperone GRP78/BiP confers chemoresistance to tumor-associated endothelial cells. Mol Cancer Res. 2008; 6:1268–75. [PubMed: 18708359]
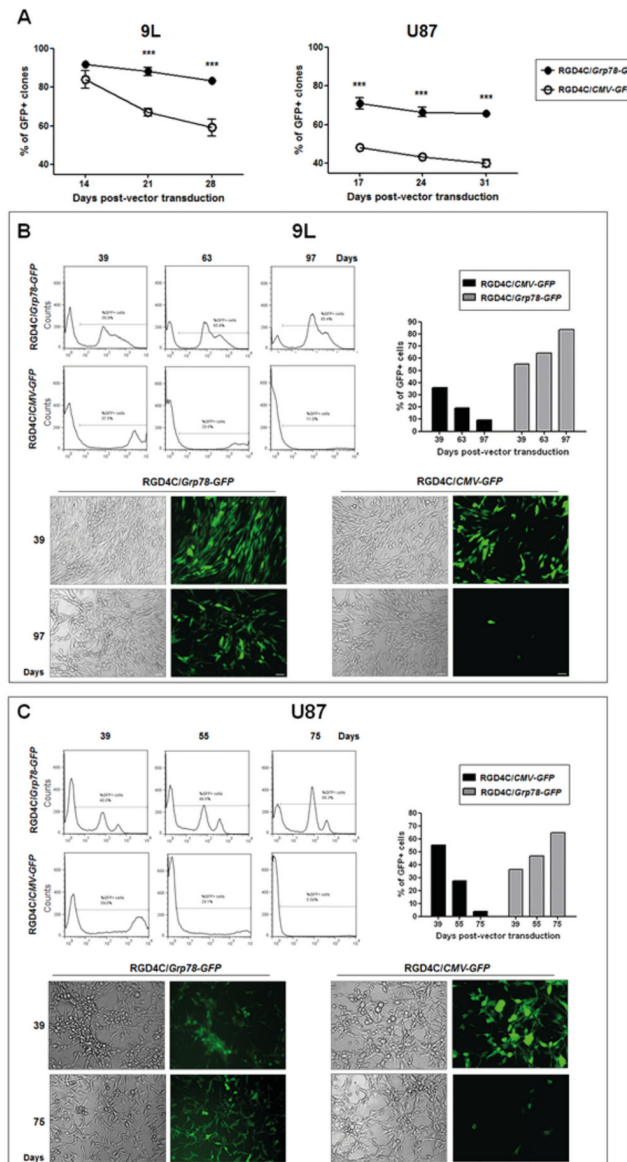
Figure 1. Persistence of *Grp78* promoter activity in glioblastoma cells upon transduction with RGD4C/*Grp78-GFP*

9L and U87 cells were transduced with either RGD4C/*Grp78-GFP-puro*[R] or RGD4C/*CMV-GFP-puro*[R]. A) At day 14 post-vector transduction, 9L and U87 puromycin resistant clones were analysed for GFP expression over time. Data are shown as percentage of GFP positive cell clones over the total number of puromycin resistant clones. B) Time course FACS analysis of GFP expression in 9L cell population of pooled cell clones. Pictures are representative of GFP positive cell change overtime. C) Similar FACS analysis of U87 cell population. Representative pictures show GFP expression overtime. Scale bar = 45 μm
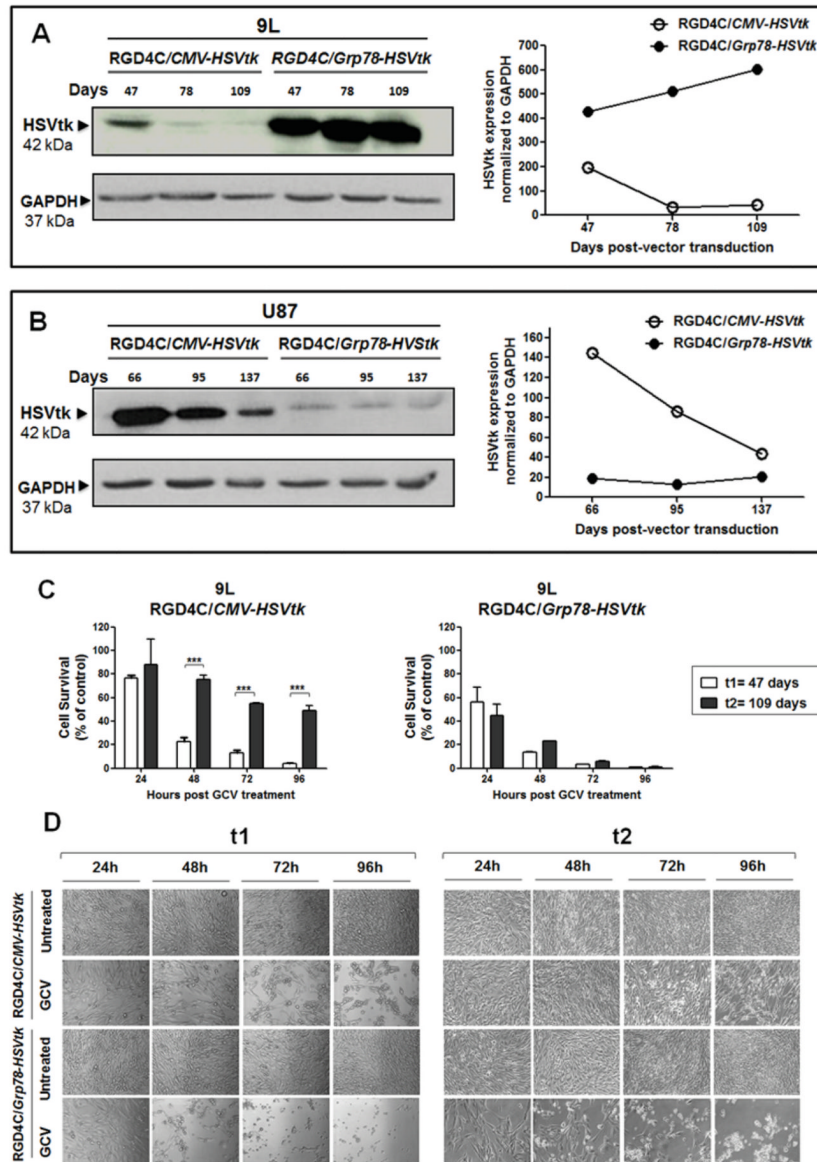
Figure 2. *HSVtk* expression and tumor cell death induction by GCV
A) 9L and B) U87 cells were stably transduced with RGD4C/*Grp78-HSVtk-puro^R* or
RGD4C/*CMV-HSVtk-puro^R* and subjected to western blot analyses at the indicated days
post-transduction. C) Evaluation of HSVtk cell killing after GCV treatment of 9L cells at
days 47 and 109 post-transduction. Cells were counted in triplicate for each condition in 24
hr intervals over 96 hr post GCV treatment. Data were calculated by dividing the percent
conversion under GCV condition by that under non-GCV condition. Data represent the
mean obtained from triplicate wells. D) Representative phase contrast images of 9L cells at
47 and 109 days post-transduction and following GCV treatment for 24, 48, 72 or 96 hr.
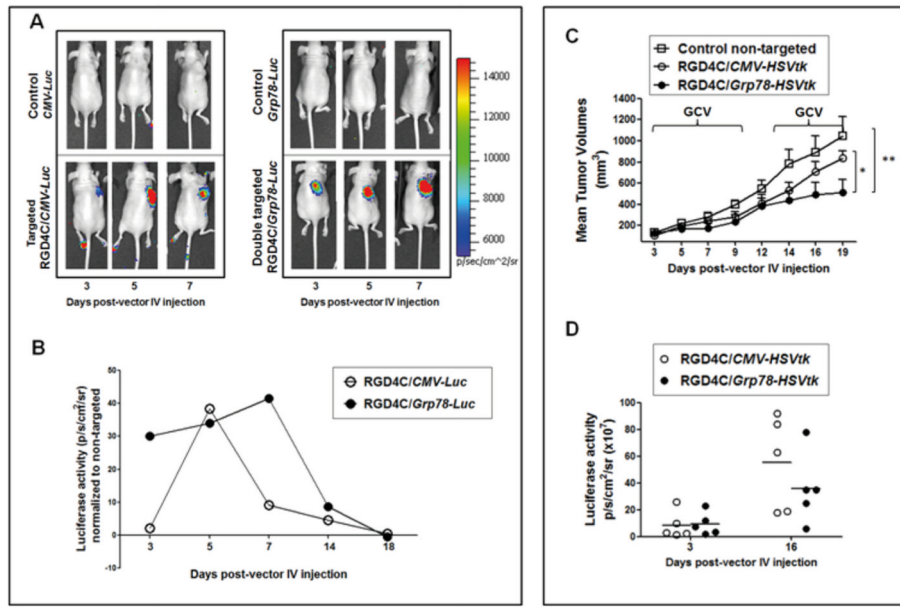
Figure 3. Systemic administration of RGD4C/*Grp78* mediates efficient *Luc* expression in 9L tumors, and achieves therapy with *HSVtk* plus GCV

A) *In vivo* BLI of *Luc* in tumor-bearing mice. Nude mice with 9L xenografts (~100 mm^3) received a single intravenous dose of RGD4C/*Grp78-Luc*, RGD4C/*CMV-Luc* or control insertless vectors. A standard calibration scale is provided. B) Serial real-time quantification of *Luc* expression in tumors. *Luc* expression from targeted vectors was normalised to that of control non-targeted. C) Growth curves of tumors after intravenous administration of *HSVtk*-expressing vectors. GCV was injected to mice from post-vector delivery day 3 until day 10, then re-administered from day 13 until the end of experiments. Shown are the mean tumor volumes. D) Changes in tumor viability before and after GCV therapy as assessed with BLI of *Luc* expression. Tumors were established in nude mice by implantation of 9L cells stably expressing the *Luc* transgene.
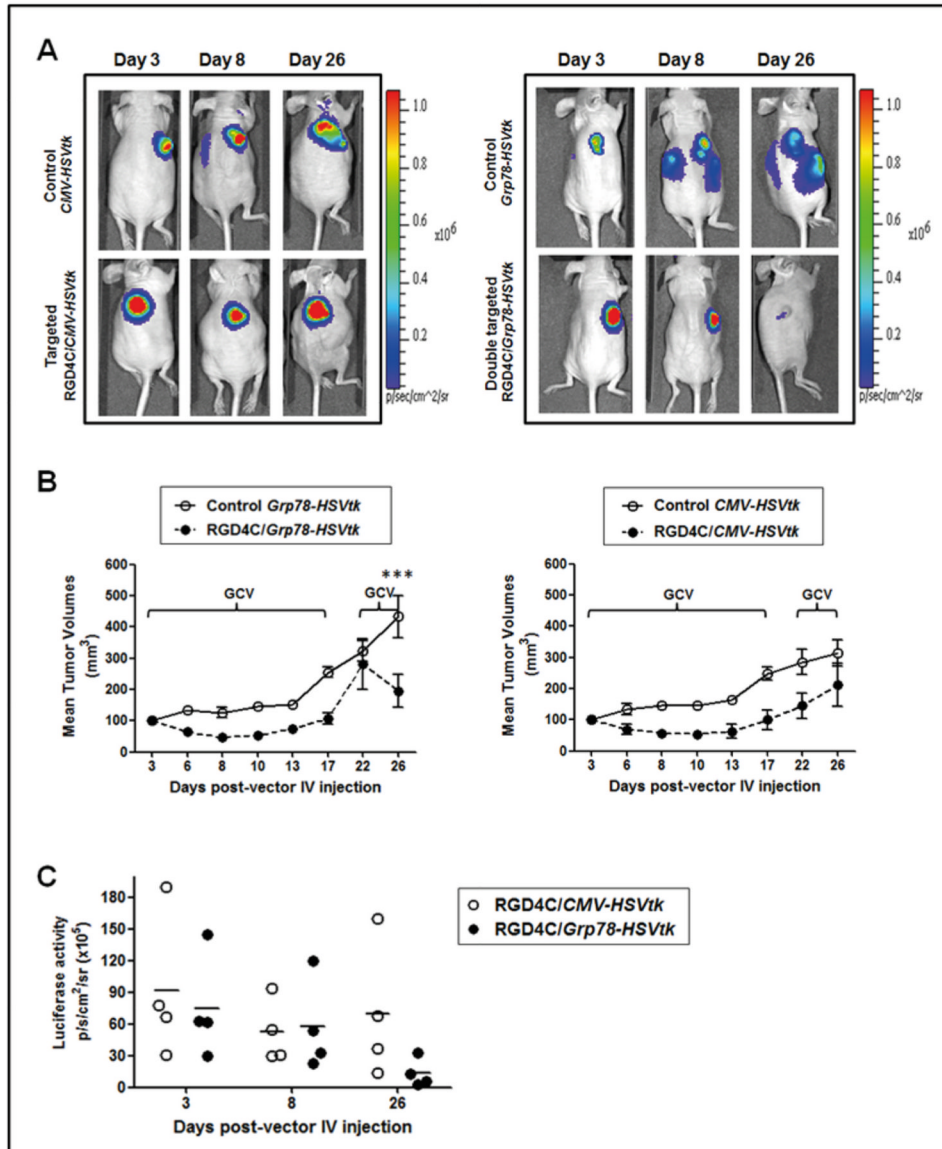
Figure 4. Therapeutic efficacy of RGD4C/*Grp78-HSVtk* in U87 glioblastoma
Nude mice bearing U87 xenografts, derived from *Luc*-expressing U87 cells, were
intravenously administered with RGD4C/*Grp78-HSVtk*, RGD4C/*CMV-HSVtk* or control
vectors. GCV treatment started when tumors reached ~100 mm³ and was given daily until
day 17 post-vector delivery then re-administered at day 22. A) Representative images of BLI
showing tumor size and tumor viability as visualised by *Luc* activity at the indicated days
post-vector administration. B) Tumor growth curves after GCV treatment. C) Changes in
tumor viability before and after GCV treatment as measured by BLI of tumor *Luc* activity.
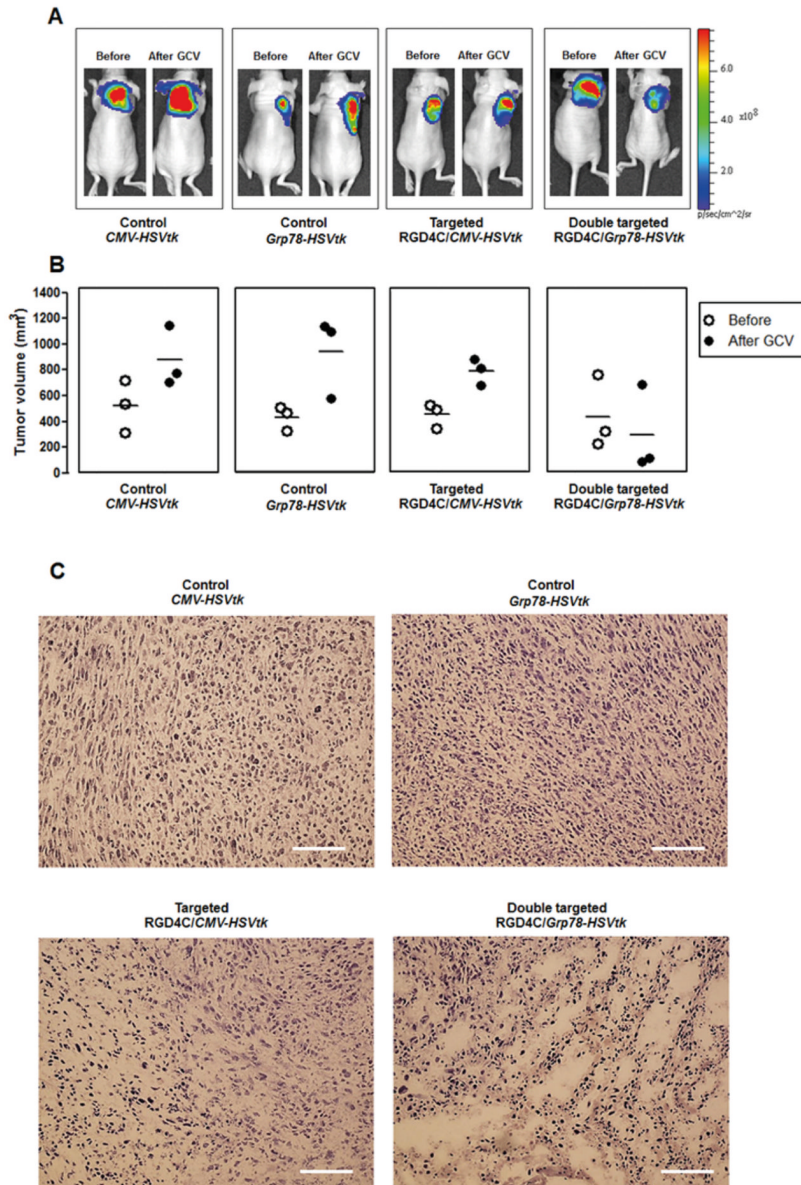
Figure 5. Regression of large 9L tumors by RGD4C/*Grp78-HSVtk* plus GCV
A) Representative tumor-bearing mice from all experimental groups before and after GCV therapy. Mice were implanted with 9L cells stably expressing the *Luc* transgene under the *Grp78* promoter. Next, mice bearing 9L xenografts received an intravenous dose of RGD4C/*Grp78-HSVtk*, RGD4C/*CMV-HSVtk*, or control insertless vectors. GCV was administered to mice at day 3 post-vector delivery (tumor size ~400-450 mm^3) and continued for 5 days. *Luc* expression was monitored before and after GCV treatment. B) Individual tumor volumes are represented before (open circles) and after (filled circles) GCV treatment. C) H&E staining of representative tumor sections from all experimental groups.
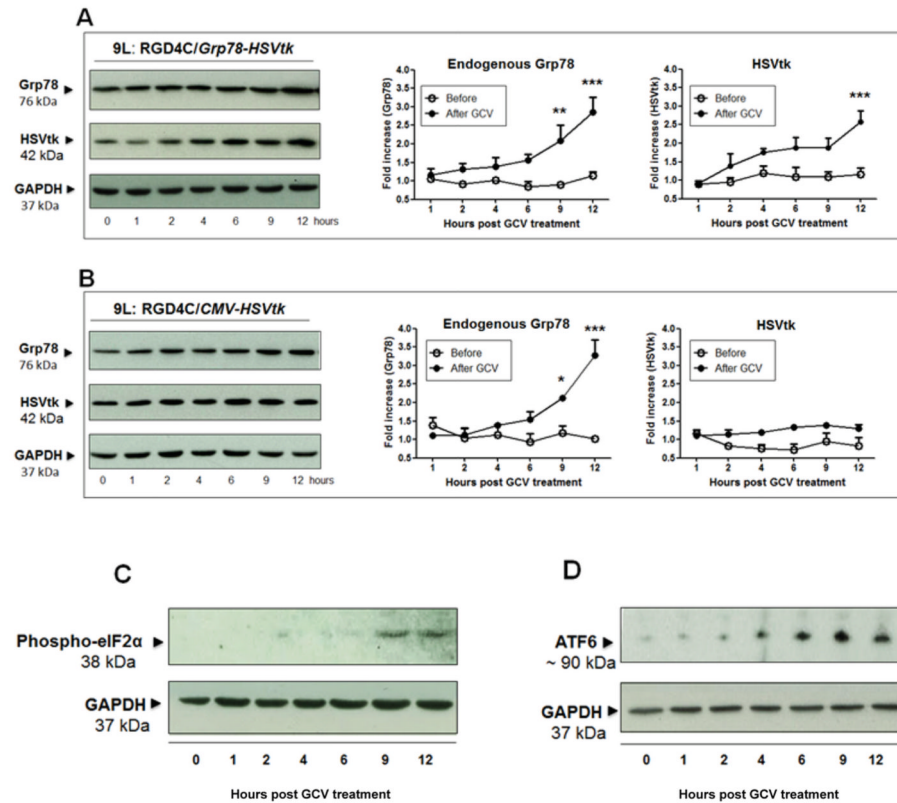
Figure 6. Combination of HSVtk expression and GCV induces *Grp78* promoter
9L cells stably transduced with (A) RGD4C/*Grp78-HSVtk* or (B) RGD4C/*CMV-HSVtk*
were treated with GCV for the indicated times, then subjected to western blot analyses with
antibodies against Grp78, HSVtk and GAPDH as control. Endogenous Grp78 and HSVtk
levels were measured, normalized to GAPDH and fold increase over time zero-control was
calculated for each sample (n=3). C) and D) Western blot analysis of phospho-eIF2α and
ATF6 expression, respectively.